Kearns, D. R., Mirau, P. A., Assa-Munt, N., & Behling, R. W. (1983) in *Nucleic Acids: The Vectors of Life* (Pullman, B., & Jortner, J., Eds.) pp 113-125, D. Reidel Publishing Co., Boston.

Klug, A., Jack, A., Viswamitra, M., Kennard, O., Shakked, Z., & Steitz, T. (1979) *J. Mol. Biol. 131*, 699-680.

Kumar, A., Wagner, G., Ernst, E., & Wuthrich, K. (1981) *J. Am. Chem. Soc. 103*, 3654-3658.

Leslie, A., Arnott, S., Chandrasekaran, R., & Ratliff, R. (1980) *J. Mol. Biol. 143*, 49-72.

Mitsui, Y., Langridge, R., Shortle, B., Cantor, C., Grant, R., Kodama, M., & Wells, R. (1970) *Nature (London) 228*, 1166-1169.

Nickol, J., Behe, M., & Felsenfeld, G. (1982) *Proc. Natl. Acad. Sci. U.S.A. 79*, 1771-1775.

Patel, D. J. (1978) *Eur. J. Biochem. 83*, 453-464.

Patel, D. J., Canuel, L., & Pohl, F. (1979) *Proc. Natl. Acad. Sci. U.S.A. 76*, 2508-2511.

Patel, D. J., Kozlowski, S., Norheim, A., & Rich, A. (1982) *Proc. Natl. Acad. Sci. U.S.A. 79*, 1413-1417.

Pohl, F., & Jovin, T. (1972) *J. Mol. Biol. 67*, 375-396.

Ramaswamy, N., Bansal, M., Gupta, G., & Sasisekharan, V. (1982) *Proc. Natl. Acad. Sci. U.S.A. 79*, 6109-6113.

Redfield, A., & Kuntz, S. (1979) in *NMR in Biochemistry* (Opella, S., & Lu, P., Eds.) pp 225-239, Marcel Dekker, New York.

Reid, D., Salisbury, S., & Williams, D. (1983) *Nucleic Acids Res. 11*, 3779-3793.

States, D., Haberkorn, R., & Ruben, D. (1982) *J. Magn. Reson. 48*, 286-292.

Sutherland, J., & Griffin, K. (1983) *Biopolymers 22*, 1445-1448.

Thamann, T., Lord, R., Wang, A., & Rich, A. (1981) *Nucleic Acids Res. 9*, 5443-5457.

Tran-Dinh, S., Neumann, J., Huynh-Dinh, T., Genissel, B., Igolen, J., & Simonnot, G. (1982) *Eur. J. Biochem. 124*, 415-425.

van de Sande, J., & Jovin, T. (1982) *EMBO J. 1*, 115-120.

Wagner, G., & Wuthrich, K. (1979) *J. Magn. Reson. 33*, 675-680.

Wang, A., Quigley, G., Kolpak, F., van der Marel, G., van Boom, J., & Rich, A. (1979) *Nature (London) 282*, 680-686.

Wells, R. D., Goodman, T., Hillen, W., Horn, G., Klein, R., Larson, J., Muller, U., Neuendorf, S., Panayotatos, N., & Stirdivant, S. (1980) *Prog. Nucleic Acid Res. Mol. Biol. 24*, 167-267.

Wright, J. M., Feigon, J., Denny, W. A., Leupin, W., & Kearns, D. R. (1981) *J. Magn. Reson. 45*, 514-519.

Zimmer, C., Tymen, S., Marck, C., & Guschlbauer, W. (1982) *Nucleic Acids Res. 10*, 1081-1091.

Kinetic Mechanism in the Direction of Oxidative Decarboxylation for NAD-Malic Enzyme from *Ascaris suum*†

Sang-Hoon Park, Dennis M. Kiick, Ben G. Harris, and Paul F. Cook*

ABSTRACT: Measurement of the initial rate of the malic enzyme reaction varying the concentration of NAD at several different fixed levels of Mg^{2+} (0.25-1.0 mM) and a single malate concentration gave a pattern which intersects to the left of the ordinate. Repetition of this initial velocity pattern at several additional malate concentrations and treatment in terms of a terreactant mechanism suggests an ordered mechanism in which NAD adds prior to Mg^{2+} which must add prior to malate. On the other hand, when a broader concentration range of Mg^{2+} (0.25-50 mM) is used, data are consistent with a random mechanism in which Mg^{2+} must add prior to malate. By use of product inhibition studies, pyruvate is competitive vs. malate and noncompetitive vs. NAD, while NADH is competitive vs. NAD and noncompetitive vs. malate. These results are consistent with the random addition of substrates and further suggest rapid equilibrium random release of products. Tartronate, a dead-end analogue of malate, is competitive vs. malate and noncompetitive vs. NAD. Thio-NAD is a slow substrate which is used at 2.4% the maximum rate of NAD. When used as a dead-end analogue of NAD, thio-NAD is competitive vs. NAD and gives a complex inhibition pattern vs. malate in which competitive inhibition is apparent at low concentrations of malate (<12.5 mM), and this changes to uncompetitive inhibition at high concentrations of malate (>12.5 mM). These data are consistent with a steady-state random mechanism in the direction of oxidative decarboxylation in which Mg^{2+} adds in rapid equilibrium prior to malate. However, calculations based on intracellular levels of substrates suggest that the ordered mechanism discussed above probably operates under physiologic conditions.

The NAD-malic enzyme from *Ascaris suum* catalyzes the oxidative decarboxylation of L-malate. Initial velocity and isotope partitioning studies suggest that, with Mn^{2+} as the divalent metal ion, the enzyme has a random kinetic mechanism in the forward direction in which either malate or NAD can bind to the enzyme-Mn^{2+} complex (Landsperger et al., 1978). Thus, the kinetic mechansim of this enzyme appears to be quite distinct from the ordered sequential mechanism of the pigeon liver NADP-malic enzyme (Hsu & Lardy, 1967; Schimerlik & Cleland, 1977).

Very little is known of the extended mechanism, however (including the metal as a pseudoreactant), for either of the above enzymes. All previous studies on the *Ascaris* malic

† From the Department of Biochemistry and Chemistry, North Texas State University/Texas College of Osteopathic Medicine, Denton, Texas 76203. *Received March 9, 1984.* This research was supported by National Institutes of Health Grants AI-12331 (B.G.H.) and GM 31686 (P.F.C.), an Organized Faculty Research Grant (P.F.C.) from the Texas College of Osteopathic Medicine, and BRSG S07 RR07195-03 (P.F.C.) awarded by the Biomedical Research Grant Program, Division of Research Resources, National Institutes of Health. P.F.C. is the recipient of a NIH Research Career Development Award (AM 01155).

0006-2960/84/0423-5446$01.50/0

enzyme maintained the metal concentration constant (Landsperger et al., 1978). Metal saturation curves have been obtained for a number of malic enzymes (Milne & Cook, 1979; Brown & Cook, 1981; Yamaguchi et al., 1973, 1974; Grover et al., 1981; Schimerlik et al., 1977), and in several cases, the saturation curves for other reactants, particularly malate and NAD, were determined with two separate metals (Milne & Cook, 1979; Brown & Cook, 1981; Yamaguchi et al., 1974). However, studies were not thorough enough to determine potential randomness of addition of metal and reactant. Lapis & Harrison (1978) showed rapid equilibrium ordered addition of Mg^{2+} and malate for the porcine heart mitochondrial enzyme, while the pigeon liver enzyme was shown to allow random addition of metal and nucleotide (Hsu et al., 1976; Pry & Hsu, 1980).

In view of the diversity in mechanism for this enzyme dependent on the source from which it is obtained, it is of interest to elucidate the kinetic mechanism for the NAD–malic enzyme from *Ascaris suum*. This report deals with an elucidation of the kinetic mechanism in the direction of oxidative decarboxylation of malate including the divalent metal ion (Mg^{2+}) as a pseudoreactant. The result of initial velocity studies in the absence and presence of products and dead-end inhibitors suggests that the kinetic mechanism is fully random. However, it is also established that, with the use of narrow ranges of substrate concentrations in the initial velocity studies, the kinetic mechanism appears to be ordered. It is suggested that the ordered mechanism prevails in vivo.

Materials and Methods

Chemicals and Enzymes. *Ascaris suum* malic enzyme was purified according to Allen & Harris (1981). Enzyme was homogeneous by the criterion of SDS[1]–polyacrylamide gel electrophoresis run according to the method of O'Farrell (1975) as modified by Atkins et al. (1975). Enzyme has a subunit molecular weight of 65 000 and a final specific activity of 40 units/mg assayed according to Allen & Harris (1981). All other reagents and chemicals were obtained from commercially available sources and were of the highest quality available.

Initial Velocity Studies. These studies were carried out on a Gilford 2600 spectrophotometer to monitor the absorbance of 340 nm due to the appearance of NADH. All assays were run at 25 °C, and the temperature was maintained with a circulating water bath with the capacity to heat and cool the thermospacers of the Gilford. Reaction cuvettes were 1 cm in path length and 1 or 3 mL in volume. All cuvettes were incubated for at least 10 min in the water bath and 5 min in the cell compartment prior to initiation of reaction. Temperatures were routinely monitored with a YSI Tele thermometer. A typical assay contained 100 mM buffer (see pH studies), 1 mM DTT, variable concentrations of divalent metal, malate, and NAD, and 8.4 nM malic enzyme. All assays reflected initial velocity conditions with less than 10% of the limiting reactant utilized over the time course of the reaction. Initial velocity patterns (e.g., at pH 9.0, 100 mM Taps) were obtained by varying the uncomplexed NAD concentration[2] from 20 μM to 2 mM at Mg_f^{2+} levels of 0.25, 0.37, 0.68, 5, and 50 mM and a fixed $malate_f$ concentration of 10 mM. This pattern was then repeated at $malate_f$ concentrations of 14.3, 25, and 100 mM.

Metal Chelate Correction. The concentration of the reactants malate and NAD added to the reaction mixture were corrected for the concentration of the metal–ligand chelate complex. The total concentration of any reactant was calculated according to the following equation:

$$[L]_t = [L]_f + \frac{[L]_f[M^{2+}]_f}{K_{ML}} \quad (1)$$

where $[L]_t$ is the total final concentration of ligand added to the reaction mixture, $[L]_f$ is the desired uncomplexed concentration of the ligand, $[M^{2+}]_f$ is the desired uncomplexed concentration of divalent metal, and K_{ML} is the equilibrium constant for dissociation of the metal–ligand chelate complex [K_{ML} = (M)(L)/(ML)]. The total concentration of divalent metal to be added under any given set of concentration conditions for a solution containing i ligands was calculated according to the following equation:

$$[M^{2+}]_t = [M^{2+}]_f + \sum \frac{[M^{2+}]_f[L_i]_f}{K_{ML_i}} \quad (2)$$

where $[M^{2+}]_t$ is the total final concentration of divalent metal to be added to the reaction mixture, $[L_i]_f$ is the desired uncomplexed concentration of the ith ligand, K_{ML_i} is the equilibrium constant for dissociation of a chelate complex between divalent metal and the ith ligand, and $[M^{2+}]_f$ has the same definition as above.

Dissociation constants used in the above calculations are the following: Mg–malate, 25.1 mM; Mg–NAD, 19.5 mM; Mg–MES, 160 mM; Mg–pyruvate, 158.5 mM; Mg–tartronate, 6.8 mM (Martell & Smith, 1977; Good et al., 1966). The dissociation constant for Mg–thio-NAD was assumed the same as Mg–NAD. All other reaction components gave negligible corrections under concentration conditions used.

pH Studies. The initial velocity patterns used to obtain information on the kinetic mechanism were determined at pH values 7.0 (Hepes) and 9.0 (Taps) as described under Initial Velocity Studies. This served to provide values for all kinetic parameters over a pH range and thus give the pH dependence for the kinetic mechanism over this pH range. Since total malate concentrations were somewhat high in some cases (particularly low pH), malate was titrated to the approximate pH value of the assay. Above pH 9, NAD was added to the reaction mixture just prior to the addition of enzyme to minimize the base-catalyzed degradation of the nucleotide. The pH of the reaction mixture was recorded before and after sufficient data were collected for determination of initial velocities. In all cases, pH change was negligible before and after reaction. No significant effect of ionic strength was observed up to 3.5 M.

Data Processing. Reciprocal initial velocities were plotted vs. reciprocal substrate concentrations. Data were fitted to the appropriate rate equations whenever possible by using the Fortran programs of Cleland (1979). Data conforming to rapid equilibrium ordered addition of the metal prior to malate were fitted to eq 3, while data conforming to a general se-

[1] Abbreviations: SDS, sodium dodecyl sulfate; DTT, dithiothreitol; Mes, 2-(*N*-morpholino)ethanesulfonic acid; Pipes, piperazine-*N*,*N*′-bis-(2-ethanesulfonic acid); Hepes, *N*-(2-hydroxyethyl)piperazine-*N*′-2-ethanesulfonic acid; Taps, 3-[[tris(hydroxymethyl)methyl]amino]-propanesulfonic acid; Ches, 2-(*N*-cyclohexylamino)ethanesulfonic acid; Caps, 3-(cyclohexylamino)-1-propanesulfonic acid.

[2] The chelate complexes Mg–NAD and Mg–malate are not substrates for this enzyme as will be shown. Instead, the uncomplexed form of both reactants and the metal are required. We suggest using Mg_f^{2+}, NAD_f, and $malate_f$ to represent the concentrations of Mg^{2+}, NAD, and malate, respectively, which have been corrected for the concentration of the chelate complexes.

quential equation were fit to eq 4. Terreactant initial velocity data were first analyzed graphically according to Viola & Cleland (1982). As a result, the presence or absence of several terms in the denominator of the rate equation for a fully random terreactant mechanism was questioned. Data were then fitted to eq 5 which describes a fully random mechanism, confirming whether terms were defined or undefined. For data with Mg^{2+} varied from 0.25 to 1 mM, eq 6 was used, which describes an ordered mechanism in which B adds in rapid equilibrium. Data for competitive, noncompetitive, and uncompetitive inhibition were fitted to eq 7–9.

$$v = \frac{VAB}{K_{ia}K_b + K_bA + AB} \quad (3)$$

$$v = \frac{VAB}{K_{ia}K_b + K_aB + K_bA + AB} \quad (4)$$

$$v = VABC/[\text{constant} + (\text{coef } A)A + (\text{coef } B)B + (\text{coef } C)C + K_aBC + K_bAC + K_cAB + ABC] \quad (5)$$

$$v = \frac{VABC}{\text{constant} + (\text{coef } A)A + K_aBC + K_cAB + ABC} \quad (6)$$

$$v = \frac{VA}{K_a(1 + I/K_{is}) + A} \quad (7)$$

$$v = \frac{VA}{K_a(1 + I/K_{is}) + A(1 + I/K_{ii})} \quad (8)$$

$$v = \frac{VA}{K_a + A(1 + I/K_{ii})} \quad (9)$$

In eq 3–9, A, B, and C are reactant concentrations, and I is inhibitor concentration; K_a, K_b, and K_c are Michaelis constants, and K_{ia}, K_{is}, and K_{ii} are inhibition constants for A, slope, and intercept, respectively. The constant and coefficient terms are lumped kinetic constants which are dependent on mechanism. These will be discussed in terms of malic enzyme under Discussion.

Results

Reactants in the Direction of Oxidative Decarboxylation. Since the NAD–malic enzyme from *Ascaris suum* requires a divalent metal ion for activity, it is important to determine whether uncomplexed metal or the metal–reactant chelate complex is the true substrate. The following should be considered. First, when reciprocal velocity is plotted vs. reciprocal of total malate at constant NAD and Mg^{2+} concentrations, parabolic plots are obtained. However, if data are corrected for the amount of chelate complex and uncomplexed malate is plotted, the reciprocal plots are linear. This is in agreement with data reported by Canellas & Wedding (1980) for the NAD–malic enzyme from cauliflower. Second, an initial velocity pattern (16 data points) was obtained by varying malate at several different fixed levels of Mg^{2+}. Data were then plotted in reciprocal form vs. concentrations of the Mg–malate complex or uncomplexed concentrations of Mg^{2+} and malate. If Mg–malate is the reactant, all 16 points should fall on a single line, whereas if the uncomplexed species are reactants, a series of straight lines will be obtained for $1/v$ vs. $1/[\text{malate}]$ for each of four Mg^{2+} concentrations. The latter is observed, consistent with uncomplexed reactants as substrates. Moreover, the pattern obtained intersects on the ordinate indicative of rapid equilibrium ordered addition of Mg^{2+} prior to malate (confirmed by fit to eq 3). Third, the concentration of malate was fixed at 1 mM (K_{malate}), and the Mg^{2+} concentration was increased from a concentration where virtually no Mg–malate complex was present to a point where greater than 95% of the malate was complexed. In this case, the rate first increased and then decreased continually to about zero, mimicking substrate inhibition. These data are consistent with uncomplexed Mg^{2+} and malate as reactants, but they do not provide information on whether Mg–malate is inhibitory. When the reciprocal experiment is carried out, however, with Mg^{2+} fixed at 1 mM and the concentration of malate increased, the rate increases as a hyperbolic function of malate. These data are consistent with the rapid equilibrium ordered addition of Mg^{2+} prior to malate[3] and effectively rule out inhibition by Mg–malate. Thus, all reactant concentrations were corrected for the concentration of the chelate complex, and the malic enzyme reaction was treated as a pseudoterreactant reaction. The above experiments were repeated at pH 7.3 with identical results.

Table I: Kinetic Constants at pH 7 and 9 for the NAD–Mg^{2+}–Malate Initial Velocity Pattern Using a Narrow Range of Mg^{2+} and NAD Concentrations[a]

parameter	value ± SE[b] pH 7.0	pH 9.0
V	18.5 ± 4.6	14.5 ± 0.9 μM/min
K_A	57 ± 36	90.1 ± 14.9 μM
K_C	78 ± 35	35.9 ± 5.0 mM
coef A	23 ± 12	10.2 ± 2.5 mM^2
constant	3.2 ± 1.0	4.1 ± 0.3 mM^3
K_{iA}	0.13 ± 0.09	0.41 ± 0.1 mM
K_{IB}	0.30 ± 0.16	0.28 ± 0.08 mM

[a] Buffer: pH 9, Ches; pH 7.0, Hepes. All assays contained 100 mM buffer and 0.038 unit of malic enzyme in cuvettes with a 1.0-cm light path and 1.0 or 3.0 mL volume. NAD_f (A) concentrations were 0.05, 0.071, 0.125, and 0.5 mM; Mg_f^{2+} (B) concentrations were 0.25, 0.33, 0.5, and 1.0 mM; $malate_f$ (C) concentrations were 10.0, 14.3, 25.0, and 100.0 mM. [b] Data were fitted to eq 6. The constant and coef A terms are lumped constants which were defined by deriving the mechanism by using the method of Cha (1968). Constant = $K_{ia}K_{Ib}K_c$ and coef A = $K_{Ib}K_c$ where K_{ia} is the dissociation constant for EA and K_{Ib} is the dissociation constant for B from EAB.

Initial Velocity Studies in the Absence of Inhibitors. Initial velocities were obtained at a fixed concentration of $malate_f$, varying the concentration of NAD_f at several different fixed levels of Mg_f^{2+}. This experiment was then repeated at three additional levels of malate. All data were then fitted first to the equation for a completely random terreactant mechanism (eq 5) and then to the equation for ordered addition with B adding in rapid equilibrium (eq 6). Values for the fitted parameters are shown in Table I. All of the above experiments were repeated at pH 7.3 with qualitatively identical results. In all three cases, the (coef Mg), (coef malate), and K_{Mg} terms were undefined. Kinetic parameters are shown in Table I.

Since the above studies were carried out using a narrow concentration range of some of the reactants, the above experiments were repeated at pH 9 using broad concentration ranges. These data are shown in Figure 1. Unlike the data obtained with narrow concentration ranges, when broader concentration ranges are used, some of the replots, Figures 2 and 3, are curved. In addition, the tertiary replots (Figure 3) indicate that all terms except K_{Mg} are present in the denominator of the rate equation for a fully random terreactant mechanism. The secondary slope vs. $1/Mg_f^{2+}$ replot (Figure 2) suggests that the Mg_f^{2+} saturation curve is biphasic under conditions when NAD_f is maintained at low levels, regardless of the malate level. To check this finding, the saturation curve for Mg_f^{2+} was repeated by using these conditions. As shown

[3] The formation and dissociation of Mg–malate is also a rapid equilibrium process.

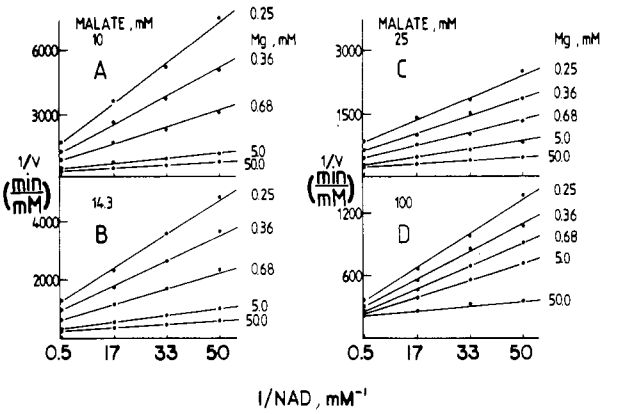

FIGURE 1: Dependence of the initial rate of the malic enzyme reaction on the concentrations of NAD_f, Mg_f^{2+}, and $malate_f$ at pH 9.0. Concentrations of NAD_f are 0.02, 0.03, 0.059, and 2.0 mM, while concentrations of Mg_f^{2+} are 0.25, 0.366, 0.68, 5, and 50 mM for A, B, C, and D. $Malate_f$ concentrations are: (A) 10, (B) 14.3, (C) 25, and (D) 100 mM. Curves are drawn by eye.

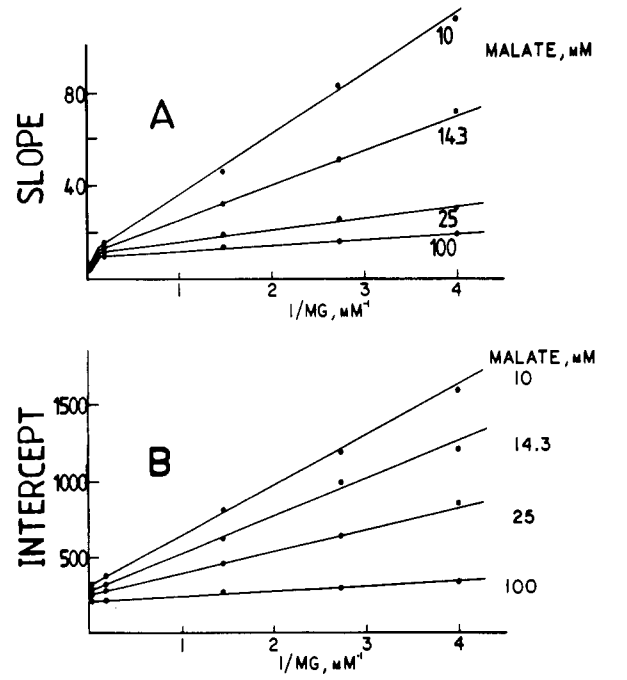

FIGURE 2: Replot of slopes (A) and intercepts (B) from Figure 1 vs. the reciprocal of Mg_f^{2+} concentration at each of the four malate concentrations used. Data in (B) were fit to eq 4.

in Figure 4, the saturation curve is indeed biphasic. Results are summarized in Table II.

On the other hand, when a similar experiment was carried out at pH 7.3 using 0.05–0.5 mM NAD_f, 25–100 mM Mg_f^{2+}, and 0.5–5 mM $malate_f$, both the E–malate and E–NAD–malate terms were not present. Thus, even though a wide range of concentrations was used, the binding of malate to free enzyme was not observed. This does not necessarily indicate that the complex does not form but rather that the malate concentration may not be high enough to observe this complex.[4] However, unlike the data obtained by using a low range of Mg_f^{2+} concentrations, the E–Mg term is present. In addition, unlike the data obtained at pH 9, there is no apparent curvature in the replots. This may be a result of the concentration of Mg_f^{2+} not being increased to high enough levels. Results are summarized in Table II.

[4] Evidence will be presented in the following paper (Kiick et al., 1984) on the presence of E–NAD–malate.

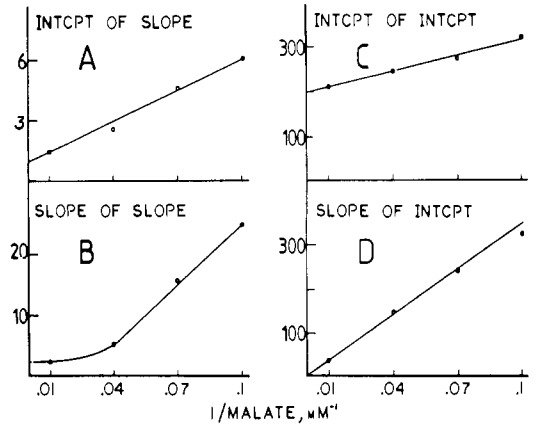

FIGURE 3: Replots of intercepts (A) and slopes (B) from Figure 2A vs. the reciprocal of $malate_f$ concentration. Replots of intercepts (C) and slopes (D) from Figure 2B vs. the reciprocal of malate concentration.

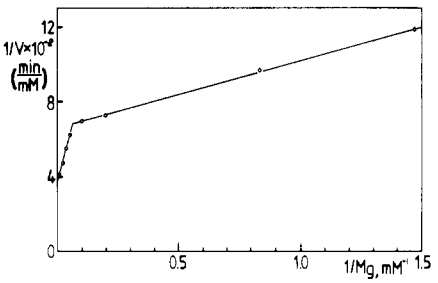

FIGURE 4: Dependence of the initial rate of the malic enzyme reaction on Mg_f^{2+} concentration at pH 9.0. The concentrations of NAD_f and $malate_f$ were maintained at 0.02 and 25 mM, respectively. The curve is the best eye fit to the data.

Table II: Kinetic Constants for NAD–Malic Enzyme from *Ascaris suum* at pH 7.3 and 9.0[a]

parameter	value ± SE	
	pH 7.3	pH 9.0
V	13.2 ± 0.6	14.7 ± 0.6 μM/min
K_{malate}	1.18 ± 0.006	5.2 ± 0.6 mM
K_{NAD}	0.011 ± 0.001	0.004 ± 0.001 mM
(coef NAD)[b]	16.68 ± 0.09	16.2 ± 0.9 mM^2
(coef Mg)	0.0022 ± 0.0006	0.25 ± 0.02 mM^2
(coef malate)		0.011 ± 0.002 mM^2
constant	1.32 ± 0.006	0.15 ± 0.03 mM^3

[a] All initial velocities were obtained at 25 °C as described under Materials and Methods. Constants are extracted from a fit of the data in Figure 3 as discussed under Materials and Methods. Concentration ranges for reactants at 100 mM Taps, pH 9, are the following: NAD_f, 0.02–2 mM; Mg_f^{2+}, 0.25–50 mM; $malate_f$, 10–100 mM. At 100 mM Hepes, pH 7.3, concentrations are the following: NAD_f, 0.05–0.5 mM; Mg_f^{2+}, 25–100 mM; $malate_f$, 0.5–5 mM. All reactants were corrected for chelate complex formation. Data were fitted to eq 5. Only terms which were defined are presented. The resultant rate equation for the pH 9 data, once undefined terms were eliminated and the constant and coefficient terms were defined as in the legend of Table I, is eq 12. Similarly, the pH 7.3 data also adhere to eq 12 with the $K_{ia}K_{Ib}K_c/K_{Ic}$ term absent. The K_{Ic} term represents the dissociation constant for C from EBC. [b] The K_i for Mg^{2+} from E–NAD–Mg can be estimated from the ratio of (coef NAD) to K_{malate}. This value is 14 ■ 1 mM and 3.0 ± 0.4 mM at pH 7.3 and 9, respectively.

Product Inhibition. It is apparent from the above results that two possible kinetic mechanisms exist for the malic enzyme, random or ordered, dependent on the Mg^{2+} concentration. In order to obtain further information on the mechanism, product inhibition by $NADH_f$ and $pyruvate_f$ was determined. With NAD_f as the variable reactant, $NADH_f$ is competitve whether Mg_f^{2+} and $malate_f$ are maintained at low levels or at saturating levels. In addition, $NADH_f$ is com-

Table III: Product Inhibition Patterns for NAD–Malic Enzyme[a]

variable substrate	fixed substrate	product	pattern[b]	K_{is}[e]	K_{ii}[e]
NAD	Mg_f^{2+} (0.25 mM) malate (10 mM)	NADH	C	0.016 ± 0.002	
	Mg_f^{2+} (40 mM)[c] $malate_f$ (29 mM)	NADH	C	0.043 ± 0.001	
malate	Mg_f^{2+} (3 mM) NAD_f (0.05 mM)	NADH	C[d]	0.03 ± 0.005	
NAD	Mg_f^{2+} (40 mM) $malate_f$ (5 mM)	pyruvate	NC	190 ± 100	50 ± 7
malate	Mg_f^{2+} (40 mM) NAD_f (2 mM)	pyruvate	C	10.6 ± 0.9	

[a] Initial velocities were obtained as described under Materials and Methods in 100 mM Taps, at pH 9.0, 25 °C, except that the products indicated were added. All reactant and product concentrations were corrected for metal chelate complex formation. [b] All data were fitted to eq 7 and 8 for competitive (C) and noncompetitive (NC) inhibition unless otherwise indicated. [c] The lowest NAD concentration used in this experiment was 0.05 mM ($10K_{NAD}$), and as a result high concentrations of NADH were required for inhibition (up to 1 mM). Thus, 0.1-cm path length cells were used with a low enough enzyme concentration so that the initial rate could still be observed after mixing was accomplished in a test tube, and the contents were transferred to the cell prior to measurement of absorbance change. [d] Reciprocal plots were concave upward; thus, data were fitted line by line to the equation for a sigmoid curve, and the limiting values of K/V vs. NADH were fit via linear regression to give the K_{is} value. [e] All values are in mM ± SE.

petitive vs. $malate_f$ at high concentrations of NAD_f.

$Pyruvate_f$ is competitive vs. $malate_f$ whether NAD_f is saturating or maintained at K_{NAD} and is noncompetitive vs. NAD_f. Results are summarized in Table III.

Dead-End Inhibition. Tartronate, an analogue of malate, gave competitive inhibition vs. $malate_f$ and noncompetitive inhibition vs. NAD_f. As a potential analogue of NAD, ADP-ribose was tested. With NAD_f maintained at 80 μM, Mg_f^{2+} at 17 mM, and $malate_f$ at 1.3 mM, a large apparent K_i of 43 mM was obtained for ADP-ribose. Even when this

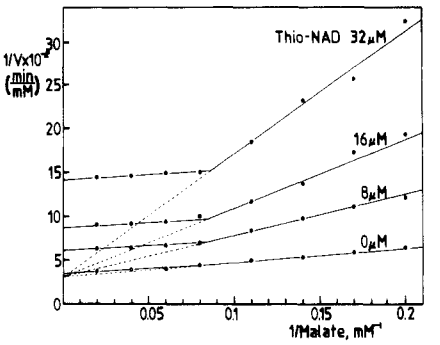

FIGURE 5: Dead-end inhibition by thio-NAD_f vs. $malate_f$ at pH 9.0. Concentration of NAD_f and Mg_f^{2+} are given in Table IV, and the $malate_f$ concentration was varied as indicated. Solid lines are a composite obtained from a fit of the data for 5–9 mM $malate_f$ to eq 7 and 12.5–50 mM $malate_f$ to eq 9. Points are experimental values. Dotted lines are an extrapolation of the theoretical curves obtained for the low malate concentration region.

K_i is corrected for lack of saturation by Mg_f^{2+} and $malate_f$, the value is ≤4 mM. Thus, the slow substrate, thio-NAD, was used as an inhibitor. At pH 9, with Mg_f^{2+} at 2.5 mM and $malate_f$ at 10 mM, thio-NAD_f gave a V_{max} 2.4% that the NAD while a K_m of 8 ± 0.1 μM was obtained. When used as an inhibitor, thio-NAD_f was competitive vs. NAD_f whether Mg_f^{2+} and $malate_f$ were maintained at K_m levels or saturating. When $malate_f$ was varied, however, complex inhibition was obtained (Figure 5). At low levels of $malate_f$, thio-NAD_f was apparently competitive vs. $malate_f$, while at saturating levels, inhibition became uncompetitive.

Chloride ion is also an inhibitor of the NAD–malic enzyme, and thus, inhibition by this ion was characterized. The anion is competitive vs. either NAD_f or $malate_f$ when the other reactants are fixed at low levels. Attempts to detect binding of chloride to the E–NAD or E–Mg–malate complexes failed. Results of dead-end inhibition patterns are summarized in Table IV.

Discussion

Reactants for Oxidative Decarboxylation. Reciprocal plots of velocity vs. malate obtained by using the concentration of total added malate are parabolic, while those using the concentrations of uncomplexed malate are linear. When data obtained varying both Mg^{2+} and malate are plotted in reciprocal form by using the concentration of the chelate complex, Mg–malate, all data do not fall on a single straight line. These

Table IV: Dead-End Inhibition Patterns for NAD–Malic Enzyme[a]

variable substrate	fixed substrate	inhibitor	pattern[b]	K_{is}[d]	K_{ii}[d]
NAD	Mg_f^{2+} (0.1 mM) $malate_f$ (10 mM)	tartronate	NC	20.5 ± 3.8	68 ± 14
malate	Mg_f^{2+} (2 mM) NAD_f (2 mM)	tartronate	C	9.3 ± 0.7	
NAD	Mg_f^{2+} (0.25 mM) $malate_f$ (10 mM)	thio-NAD	C	0.0061 ± 0.0005	
	Mg_f^{2+} (2.5 mM) $malate_f$ (158 mM)	thio-NAD	C	0.015 ± 0.0003	
malate	Mg_f^{2+} (2.5 mM) NAD_f (0.01 mM)	thio-NAD	C[c] UC	0.004 ± 0.0005	0.011 ± 0.0003
NAD	Mg_f^{2+} (0.25 mM) $malate_f$ (10 mM)	Cl^-	C	29 ± 2	
malate	Mg_f^{2+} (0.25 mM) NAD_f (0.1 mM)	Cl^-	C	46 ± 7	

[a] Initial velocities were obtained in 100 mM Taps, at pH 9, 25 °C, as described under Materials and Methods except that the inhibitors indicated were added. [b] All data were fitted to the equations for competitive (C) or noncompetitive (NC) inhibition unless otherwise indicated. [c] Data were fitted in two parts with the low malate concentration data fit with the equation for competitive inhibition and the high malate concentration data fit with the equation for uncompetitive inhibition. [d] All values are in mM ± SE.

experiments suggest Mg_f^{2+} and $malate_f$, and not the chelate complex, are reactants. In addition, if malate is fixed at a low level and Mg^{2+} is increased, apparent substrate inhibition is obtained by Mg^{2+}. If the reciprocal experiment is conducted, a hyperbolic increase in velocity is obtained. These experiments again suggest that Mg_f^{2+} and $malate_f$ are reactants and not Mg–malate. However, they could also suggest that free Mg^{2+} is inhibiting since only the experiment in which Mg^{2+} is increased at fixed low malate gives inhibition. As a check, if the uncomplexed Mg^{2+} concentration is increased at a given concentration of uncomplexed malate, a slight increase in the rate is observed. Thus, uncomplexed Mg^{2+} does not inhibit. The most likely explanation for the lack of inhibition obtained when Mg^{2+} was fixed at a low concentration and malate was increased is rapid equilibrium ordered addition of Mg_f^{2+} prior to $malate_f$. When NAD_f is fixed at a single concentration and $malate_f$ is varied at several fixed levels of Mg_f^{2+}, a pattern consistent with rapid equilibrium ordered addition of Mg_f^{2+} prior to $malate_f$ is obtained. Thus, the above data taken together are consistent with Mg_f^{2+} and $malate_f$ being reactants for the malic enzyme reaction, with a requirement for Mg_f^{2+} binding before $malate_f$. In addition, no inhibition by Mg–malate is observed.[5]

Interpretation of Initial Velocity Data at Low Mg_f^{2+} Levels. From a graphical analysis and fit of the data to eq 6 it was found that K_{Mg}, (coef Mg^{2+}), and (coef malate) were undefined. Data were therefore fitted to the rate equation for ordered addition of NAD_f, Mg_f^{2+}, and $malate_f$ with Mg_f^{2+} adding in rapid equilibrium. Thus, over the concentration ranges used in these studies the kinetic mechanism for malic enzyme in the direction of oxidative decarboxylation is as follows:

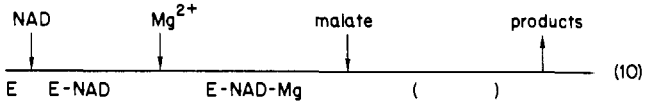

(10)

Further, since a defined K_m value is obtained for NAD, this reactant must add in steady-state rather than rapid equilibrium fashion; that is, the off-rate for NAD from E–NAD is not greater than catalysis.

Previous initial velocity studies by Landsperger et al. (1978) on this same enzyme using Mn^{2+} at a fixed concentration of 10 mM indicated a random addition of NAD and malate. This was confirmed by isotope trapping experiments by the same authors. Thus, it is possible that the mechanism changes dependent on the metal or the randomness in the kinetic mechanism could be observed with broader ranges of reactants. As a result, studies were carried out at pH 9 using a wide range of reactant concentrations to determine whether randomness could be observed.

Interpretation of Initial Velocity Data Using a Wide Range of Mg_f^{2+} and NAD_f Concentrations. Data shown in Figure 1 and Table II suggest that the mechanism for NAD–malic enzyme from *Ascaris suum* is indeed random at both pH 7.3 and pH 9.0. The tertiary replots in Figure 3 indicate that all terms are present in the denominator of the rate equation for a random terreactant mechanism except the K_{Mg} term at both pH 7.3 and pH 9.0, as well as the (coef malate) term at pH 7.3. This is in agreement with data obtained when a narrow range of Mg_f^{2+} concentrations was used (Table I). However, unlike data obtained when a narrow range of Mg_f^{2+} concentrations is used, when either Mg_f^{2+} or $malate_f$ concentrations become high enough, the E–Mg and E–malate complexes do form. There are two possibilities for the lack of the K_{Mg} term: one is that E–NAD–malate does not form at all, while the second is that Mg_f^{2+} adds in rapid equilibrium prior to the addition of malate. On the basis of the data obtained with low Mg_f^{2+} concentrations, the latter is the most likely explanation, and E–NAD–malate is dead-end.[4] This may also indicate that E–malate is also a dead-end complex. On the basis of the above, the following mechanism is suggested:

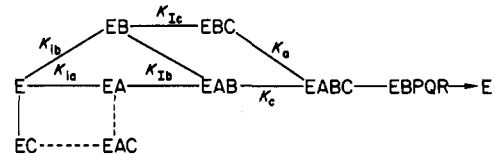

(11)

where A, B, C, P, Q, and R are NAD_f, Mg_f^{2+}, $malate_f$, CO_2, $pyruvate_f$, and $NADH_f$. Under the assumption that EC and EAC cannot add B, the rate equation for the above mechanism using the method of Cha (1968) is

$$v = VABC/[K_{ia}K_{Ib}K_c + K_{Ib}K_cA + (K_{ia}K_{Ib}K_cB/K_{ib}) + (K_{ia}K_{Ib}K_cC/K_{Ic}) + K_aBC + K_cAB + ABC \quad (12)$$

where K_i represents the dissociation constants for the binary enzyme–reactant complexes and K_{Ib} represents dissociation of the ternary EAB complex.

There is distinct curvature in some of the replots (Figures 2A and 3B) from the data shown in Figure 1. This is most likely indicative of a steady-state rather than rapid equilibrium random mechanism. In agreement is the fact that curvature is only observed at very high concentrations of reactants where one would expect the higher order terms in the rate equation to become prominent. There is reason to doubt the curvature in the secondary slope replot since this curvature is based on a single concentration. However, extensive data were obtained at 25 mM $malate_f$ by varying Mg_f^{2+} at a low NAD_f concentration with essentially identical results.

The preferred (physiologic) pathway for order of addition of reactants is most likely observed under conditions where Mg_f^{2+} is varied over a narrow range (maximum Mg_f^{2+} concentration of 1 mM). The cellular concentration of Mg_f^{2+} is on the order of 0.5 mM in rat liver (Cohen, 1983). This aspect will be discussed in more detail below. However, if malate is increased to higher concentrations, even with Mg_f^{2+} low, the pathway will switch to that in which Mg_f^{2+} addition precedes $malate_f$ which precedes NAD_f. Thus, curvature in the malate reciprocal plots is obtained when NAD_f is maintained at low levels. More evidence will be presented which is consistent with this suggestion.

Thus, when concentrations of reactants are maintained at truly saturating levels, the limiting values of K_{NAD} and K_{malate} are obtained. These values are considerably different (Table II) than those obtained for the preferred pathway (Table I). The value of K_{NAD} decreases more than an order of magnitude while K_{malate} decreases about 7-fold as Mg_f^{2+} becomes saturating.

The apparent negative cooperativity observed in the Mg_f^{2+} saturation curve is not unique to this enzyme. Cooperativity with Mn^{2+} was observed by Schimerlik et al. (1977) for the pigeon liver enzyme with apparent K_m values of 7 μM and 5 mM, respectively, for high- and low-affinity regions. These

[5] In the experiment when Mg^{2+} is fixed and malate is increased, the majority of Mg^{2+} will be complexed at high malate. No inhibition is observed under these conditions which suggests Mg–malate does not bind to malic enzyme. The increase in rate with increasing malate is simply consistent with rapid equilibrium ordered addition of Mg^{2+} prior to malate, with malate trapping the small amount of uncomplexed Mg^{2+} on enzyme.

authors also obtained data varying Mg^{2+} and observed no apparent cooperativity up to 20 mM. In addition, Milne & Cook (1979) observed positive cooperativity when Mg_f^{2+} was varied, while the saturation curve for Mn_f^{2+} was noncooperative.

Interpretation of Inhibition Data. Inhibition by $NADH_f$ is competitive vs. NAD_f whether Mg_f^{2+} and $malate_f$ are saturating or maintained at a low concentration. When $malate_f$ is varied, $NADH_f$ is also competitive when NAD_f is maintained at 50 μM ($10K_{NAD}$). The pattern becomes noncompetitive when the concentration of NAD_f is decreased. Thus, $NADH_f$ binds to free enzyme (or E–Mg) and the E–Mg–malate complex, in agreement with the random mechansim suggested by initial velocity studies alone. $Pyruvate_f$ is competitive vs. $malate_f$ when NAD_f is saturating and noncompetitive vs. NAD_f with $malate_f$ at its K_m, again in agreement with the random mechanism. Thus, $pyruvate_f$ binds to both E–Mg and E–Mg–NAD (from the intercept effect obtained from inhibition vs. NAD_f). In addition, since both products are competitive vs. the substrate of which they are an analogue when the other reactants are maintained saturating, only dead-end inhibition is obtained. Thus, unlike the suggested steady-state random mechanism in the forward direction, a rapid equilibrium mechanism is suggested in the reverse direction. In agreement with this, Landsperger et al. (1978) have reported that the ratio of the maximum rates in the forward and reverse reactions is about 30 when Mn^{2+} is used as the divalent metal. Since the off-rate for all products must be at least equal to the maximum rate in the forward direction, these rates must be at least 30 times the catalytic step in the reverse direction. Thus, the reverse reaction is predicted to be rapid equilibrium.

Further substantiation of the random mechanism is obtained from the dead-end inhibition studies. $Tartronate_f$, a dead-end analogue of malate, is competitive vs. $malate_f$ whether Mg_f^{2+} and NAD_f are maintained at low or saturating levels. When NAD_f is varied, however, $tartronate_f$ is noncompetitive. This indicates either that tartronate binds to free enzyme and NAD_f does not or that $tartronate_f$ binds to free enzyme competing with NAD_f for this form (slope effect) and also binds to the E–NAD complex (intercept effect). The latter interpretation is consistent with a random mechanism. Also consistent with the random mechanism is the complex pattern obtained by using thio-NAD_f with $malate_f$ as the variable substrate. At low concentrations of $malate_f$, there is competition between $malate_f$ and thio-NAD_f for free enzyme. However, as the concentration of $malate_f$ is increased so that most of the enzyme is present as the E–Mg–malate complex, thio-NAD_f becomes uncompetitive. These data indicate that there is some curvature in the reciprocal plot when $malate_f$ is varied, consistent with the proposed steady-state random nature of the mechanism.[6]

The K_i for thio-NAD for dissociation from the E–thio-NAD complex (6 μM) agrees well with that obtained from a fit of the low malate concentration data (4 μM) from the experiment where $malate_f$ was varied. In addition, the data for $tartronate_f$ inhibition are also internally consistent. At a saturating concentration of NAD_f, eq 12 reduces to the equation for rapid equilibrium ordered addition of Mg_f^{2+} (B) prior to $malate_f$ (C). When an inhibitor competitive with malate such as tartronate is used, this equation becomes

$$v = \frac{VBC}{K_{Ib}K_c + K_cB(1 + I/K_{is}) + BC} \quad (13)$$

where I is the $tartronate_f$ concentration and all other terms are as defined previously. At a fixed concentration of Mg_f^{2+}, with $malate_f$ varied at several different $tartronate_f$ concentrations, the slope vs. I replot will give an apparent K_i equal to the true K_i multiplied by $(1 + K_{Ib}/B)$. The value for K_{Ib} at pH 9 is 10 mM (Kiick et al., 1984) and as shown in Table IV, Mg_f^{2+} was maintained at 2 mM when $tartronate_f$ inhibition was determined by varying $malate_f$. Thus, the true K_i for $tartronate_f$ at this pH is ca. 1.5 mM. As a check of this value, the intercept effect obtained from $tartronate_f$ inhibition varying NAD_f should yield the same value. Under conditions where $malate_f$ and Mg_f^{2+} are fixed at a single concentration, the intercept is the reciprocal of eq 13, and the ${}^{app}K_{ii} = K_{ii}(1 + C/K_c + K_{Ib}/B)$. As shown in Table IV, Mg_f^{2+} and $malate_f$ were maintained at 0.1 and 10 mM, respectively. The correction term in this case is 103, and the true K_i is calculated as 0.7 mM in reasonable agreement with the calculated value of 1.5 mM.

Summary and Conclusions. Reactants in the direction of malate oxidative decarboxylation appear to be NAD_f, Mg_f^{2+}, and $malate_f$. A method of procedure is outlined for the determination of whether reactants are uncomplexed or the chelate complex and whether the chelate complex or uncomplexed reactants inhibit. This procedure is based on the apparent substrate inhibition which should be obtained when a reactant is depleted as a result of chelate complex formation by increasing the metal concentration.

Initial velocity studies in the absence of products and dead-end inhibitors give very different results dependent on the metal concentration. When the concentration of Mg_f^{2+} is maintained at low levels, the mechanism is apparently ordered with NAD_f on first followed by Mg_f^{2+} and $malate_f$. If the Mg_f^{2+} concentration range is expanded, a random mechanism is apparent except that E–NAD–malate is not productive if formed. The random mechanism suggested is most likely steady state and not rapid equilibrium since the replots do exhibit some curvature as suggested for a steady-state mechanism (Cleland, 1963). Also in agreement with the steady-state nature of the mechanism are the isotope trapping data of Landsperger et al. (1978) which suggested that E–Mn–malate and E–Mn–NAD formed and that although dissociation from the binary complexes was rapid compared to V/E_t, both reactants were sticky from the ternary complex. Product and dead-end inhibition patterns are consistent with the random nature of the reaction.

It is interesting to note that the pigeon liver NADP enzyme is highly ordered, with nucleotide adding first when Mn^{2+} is used (Hsu & Lardy, 1967; Pry & Hsu, 1980) in contrast to data obtained with the *Ascaris* enzyme. However, randomness of addition of Mn^{2+} and NADP was observed in the above mechanism (Pry & Hsu, 1980). The only other malic enzyme for which sufficient initial velocity studies have been obtained is the porcine heart mitochondrial, NADP–malic enzyme (Lapid & Harrison, 1978). Interestingly, data for this enzyme also indicate rapid equilibrium ordered addition of Mg^{2+} prior to malate. The same range of Mg^{2+} concentrations was used by these authors as was used in this study with Mg_f^{2+} varied from 0.25 to 1 mM.

The pathway that predominates at low concentrations of Mg_f^{2+} is most likely the preferred or physiologic pathway for NAD–malic enzyme. What are currently believed to be phsyiologic concentrations for reactants are the following: Mg^{2+}, 0.5 mM (Cohen, 1983); NAD, 70 μM (Barrett & Beis,

[6] This curvature almost certainly indicates switching pathways. The majority of the flux goes through the pathway with NAD bound first at low malate with a change to the pathway in which Mg^{2+} and malate bind first at high malate.

1973);[7] malate, 0.2 mM (Barrett & Beis, 1973). These concentrations are certainly consistent with addition of NAD first, followed by Mg^{2+} and malate. The flux through the malic enzyme reaction can be approximated by the flux in glucosyl residues through glycolysis from glycogen (Donahue et al., 1981). This is a value of 2–4 mM/min. The number of units of malic enzyme using 11 units/g of muscle (Payne et al., 1979) correcting for mitochondrial concentration which is 5% of the tissue weight is 234 units/mL. Thus, with the concentrations stated above and eq 12 along with the kinetic parameters in Table II, a malic enzyme activity of 0.63 mM/min is obtained, which is reasonably consistent with the flux through this enzyme.

In the following report (Kiick et al., 1984), the proposed kinetic mechanism will be tested by determining dissociation constants for as many enzyme–reactant complexes as possible. This will be done by using the sensitivity of a thiol to modification by DTNB and the modulation of this inactivation rate by reactants. Data presented in the following report (Kiick et al., 1984) agree with and support, both qualitatively and quantitatively, the kinetic mechanism proposed in this study.

Acknowledgments

We thank Rita Huber and Joye Wesley for typing the manuscript.

Registry No. NAD, 53-84-9; NADH, 58-68-4; thio-NAD, 4090-29-3; Cl, 16887-00-6; malic acid, 97-67-6; tartronic acid, 80-69-3; pyruvic acid, 127-17-3; NAD–malic enzyme, 9028-46-0.

References

Allen, B. L., & Harris, B. G. (1981) *Mol. Biochem. Parasitol. 2*, 367.

Atkins, J. F., Lewis, J. B., Anderson, C. W., & Testeland, R. E. (1975) *J. Biol. Chem. 250*, 5688.

Barrett, J., & Beis, I. (1973) *Comp. Biochem. Physiol. B 44B*, 751.

Brown, D. A., & Cook, R. A. (1981) *Biochemistry 20*, 2503.

Canellas, P. F., & Wedding, R. T. (1980) *Arch. Biochem. Biophys. 199*, 259–264.

Cha, S. (1968) *J. Biol. Chem. 243*, 820.

Cleland, W. W. (1963) *Biochim. Biophys. Acta 67*, 104.

Cleland, W. W. (1979) *Methods Enzymol. 63*, 103.

Cohen, S. M. (1983) *J. Biol. Chem. 258*, 14294.

Dawson, R. M. C., Elliott, D. C., Elliot, N. H., & Jones, K. M., Eds. (1969) *Data for Biochemical Research*, 2nd ed., p 423, Oxford University Press, London.

Donahue, M. J., Yacoub, N. J., Kaeini, M. R., Masaracchia, R. A., & Harris, B. G. (1981) *J. Parasitol. 67*, 505.

Good, N. E., Winget, G. D., Winter, W., Connolly, T. N., Izawa, S., & Singh, R. M. M. (1966) *Biochemistry 5*, 467.

Grover, S. D., Canellas, P. F., & Wedding, R. T. (1981) *Arch. Biochem. Biophys. 209*, 396.

Hsu, R. Y., & Lardy, H. A. (1967) *J. Biol. Chem. 242*, 527.

Hsu, R. Y., Mildvan, A. S., Chang, G.-G., & Fung, F. H. (1976) *J. Biol. Chem. 251*, 6574.

Kiick, D. M., Allen, B. L., Rao, J. G. S., Harris, B. G., & Cook, P. F. (1984) *Biochemistry* (following paper in this issue).

Landsperger, W. J., & Harris, B. G. (1976) *J. Biol. Chem. 251*, 3599.

Landsperger, W. J., Fodge, D. W., & Harris, B. G. (1978) *J. Biol. Chem. 253*, 1868.

Lapis, S., & Harrison, J. H. (1978) *J. Biol. Chem. 253*, 7476.

Martell, A. E., & Smith, R. M. (1977) *Critical Stability Constants*, Vol. 3, Plenum Press, New York.

Milne, J. A., & Cook, R. A. (1979) *Biochemistry 18*, 3604.

O'Farrell, P. H. (1975) *J. Biol. Chem. 250*, 4007.

Payne, D. M., Powley, D. G., & Harris, B. G. (1979) *J. Parasitol. 65*, 833.

Pry, T. A., & Hsu, R. Y. (1980) *Biochemistry 19*, 951.

Schimerlik, M. I., & Cleland, W. W. (1977) *Biochemistry 16*, 565.

Schimerlik, M. I., Grimshaw, C. E., & Cleland, W. W. (1977) *Biochemistry 16*, 571.

Viola, R. E., & Cleland, W. W. (1982) *Methods Enzymol. 87*, 353.

Yamaguchi, M., Tokushige, M., & Katsuki, H. (1973) *J. Biochem. (Tokyo) 73*, 169.

Yamaguchi, M., Tokushige, M., Takeo, K., & Katsuki, H. (1974) *J. Biochem. (Tokyo) 76*, 1259.

[7] The value of 70 μM for NAD was estimated by using the data of Barrett & Beis (1973), who obtained a value of 0.07 for the NAD/NADH ratio from the metabolite concentrations for the malic enzyme reaction. An average value for total NAD plus NADH pools is 1 mM which gives an approximate value of 0.07 mM for NAD. This will be a lower limit of the NAD concentration.